

IMAGING OF THE MAX III ELECTRON BEAM PROFILE USING VISIBLE SYNCHROTRON RADIATION

A. Hansson*, E. Wallén, Å. Andersson, MAX-lab, Lund University, SE-22100 Lund, Sweden

Abstract

The recently assembled MAX III diagnostic beam line utilizes the bending magnet synchrotron radiation (SR) in the visible to ultraviolet range to form images of the transverse electron beam profile. Computer simulations model the generation and propagation of the SR through the beam line, taking into account effects such as diffraction, the longitudinally distributed source point and the curvature of the electron orbit. Using the diagnostic beam line, the electron beam size and the emittance in the MAX III synchrotron light source has been determined.

INTRODUCTION

Several different methods are used at synchrotron light sources to determine the transverse electron beam sizes [1]. The most common methods are pinhole cameras using synchrotron radiation (SR) in the X-ray range and interferometers using SR in the visible range. Other methods are imaging with visible to ultraviolet (vis-UV) SR and X-ray imaging using focusing optics, such as a Fresnel zone plate or compound refractive lenses.

The method used at MAX III is imaging with vis-UV SR. This used to be a common method, but other methods were developed since the optical resolution of the beam imaging with vis-UV SR seemed to be insufficient for measurements of small beam sizes. However, the optical resolution can be improved by exploiting the wave-optics features of SR together with detailed modeling of the SR emission and propagation through the imaging system [2, 3].

MAX III

The MAX III synchrotron light source was commissioned in late 2006 and characterized in 2008 [4]. It is a 3rd generation electron storage ring with an electron energy of 700 MeV intended for SR generation in the infrared and ultraviolet region. It has an eightfold periodicity, 36 m circumference and a design horizontal emittance of 13 nm rad. The storage ring makes extensive use of combined function magnets to obtain a compact lattice. Each unit cell contains a dipole with a defocusing gradient and two focusing quadrupoles with a sextupole component. Two insertion devices (ID) have been installed in the ring, providing SR in the ultraviolet region. A third beam line, which will utilize infrared light from one of the dipole magnets, is currently under construction.

* anders.hansson@maxlab.lu.se

MAX III DIAGNOSTIC BEAM LINE

The MAX III diagnostic beam line was designed and installed in 2010. A detailed description of the setup of the beam line and the method used to determine the transverse electron beam profile can be found in Ref. [5].

The source point of the beam line is the center of the bending magnet in cell 6 (D6) of MAX III. The vis-UV part of the SR is reflected 90 degrees upwards by a water-cooled SiC mirror. The mirror determines the vertical acceptance of the measurement system (± 8.1 mrad). A fused silica symmetric spherical lens focuses the SR, whereas movable aperture restrictions (baffles) determine the horizontal opening angle. The SR propagates out of the vacuum system through a fused silica vacuum window. Close to the image plane, narrow band-pass filters and a Glan-Taylor polarizer select the wavelength and polarization of the measurement. At the image plane a CCD camera (pixel size $3.75 \mu\text{m}$) records the intensity distribution of the SR.

DETERMINATION OF THE ELECTRON BEAM PROFILE

Ideally, the SR intensity distribution recorded by the beam line camera would correspond to the electron beam profile at the source point scaled by the magnification factor of the system. However, features like the narrow vertical opening angle of SR and the longitudinally distributed SR generation cause the image to deviate from the scaled electron beam intensity distribution. In order to reconstruct this ideal image, the measured intensity profile is deconvoluted with the image a single electron passing through the bending magnet would give rise to at the camera. By scaling the deconvoluted (ideal) image with the magnification factor the electron beam profile at the source point is reconstructed.

The image a single electron passing through the bending magnet would give rise to at the camera is called the filament-beam-spread function (FBSF). It is calculated numerically using SRW [6]. The emission and subsequent propagation and focusing of the SR through the beam line is treated within the framework of classical electrodynamics, including in a natural way effects such as diffraction, the longitudinally distributed source point and the curvature of the electron orbit.

Figure 1 shows an example of a beam profile measurement at MAX III using σ -polarized light at 488 nm. The measured CCD camera image is shown together with the FBSF and the resulting deconvoluted image. Figure 2 shows a similar example using π -polarized light.

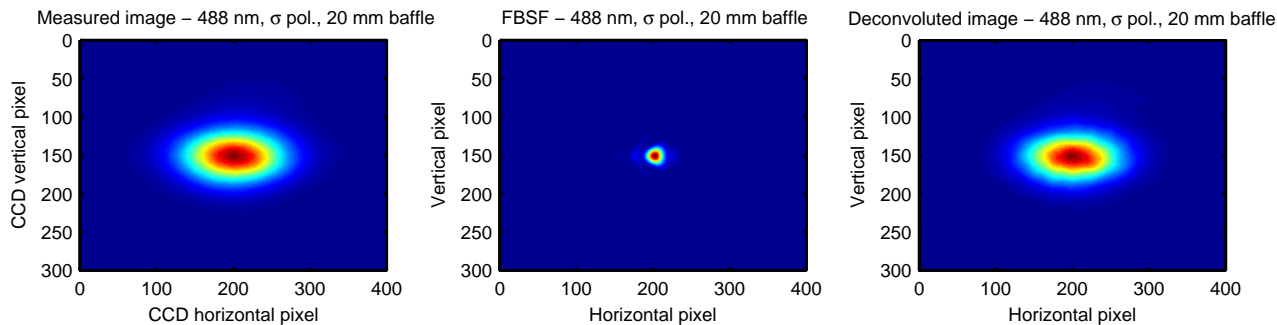


Figure 1: (Color) Example of beam profile measurement with σ -polarized light at 488 nm. Measured image, filament-beam-spread function and deconvoluted image for baffle aperture 20 mm (± 5.4 mrad horizontal opening angle).

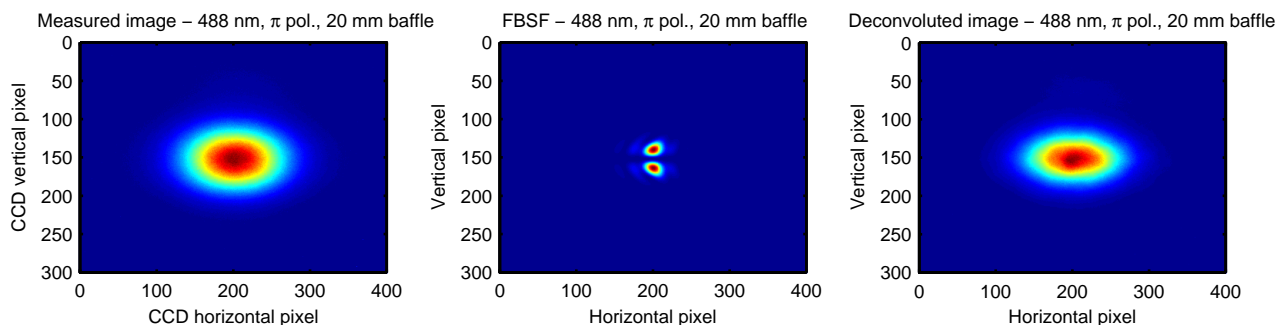


Figure 2: (Color) Example of beam profile measurement with π -polarized light at 488 nm. Measured image, filament-beam-spread function and deconvoluted image for baffle aperture 20 mm (± 5.4 mrad horizontal opening angle).

MEASUREMENTS AND RESULTS

The MAX III diagnostic beam line has been used to determine the electron beam size, dispersion and emittance in the MAX III synchrotron light source. Using MATLAB LOCO [7] the machine functions, natural energy spread, momentum compaction and horizontal emittance of a fitted MAX III lattice has been determined. The details of the measurements are given below. Table 1 shows an overview of the results obtained, comparing the design values (from Ref. [4]) with results from the fitted lattice and diagnostic beam line measurements.

Electron Beam Size

The electron beam profile in MAX III is reconstructed by scaling the deconvoluted image with the magnification factor of the measurement system. The horizontal and vertical beam sizes as well as the tilt of the electron beam ellipsis are determined by fitting a two-dimensional Gaussian to the reconstructed electron beam profile. The beam sizes in MAX III are large enough to be determined both by σ and π -polarized light. 100 images were recorded with σ -polarized light and 100 images with π -polarized light at 488 nm wavelength and 20 mm baffle aperture (± 5.4 mrad horizontal opening angle). The measurements (from which the images in Figs. 1–2 are taken) were performed at low current (1.5 mA) with the standard operating orbit in MAX III and all ID gaps open. The mean and standard deviation

of the horizontal beam size σ_x and vertical electron beam size σ_y for the 200 analyzed images were

$$\sigma_x = 101.0 \pm 0.4 \mu\text{m}$$

$$\sigma_y = 51.6 \pm 0.9 \mu\text{m}$$

The performance of the diagnostic beam line has been investigated by doing a series of measurements where the beam line configuration was varied to utilize different wavelengths and polarizations of the SR and different horizontal opening angles of the measurement system [5]. Based on that investigation and experience from operating the beam line, the standard deviation of the systematic error of the measurement is estimated to be (smaller than) 2.0 μm , which gives

$$\sigma_x = 101.0 \pm 2.0 \mu\text{m}$$

$$\sigma_y = 51.6 \pm 2.2 \mu\text{m}$$

Fitted Lattice (LOCO)

Using MATLAB LOCO [7] a computer model of the MAX III ring was fitted to 24 sets of measurement data. Three response matrix measurements were performed, with the standard operating orbit and ID gaps open, at three different occasions. At each occasion eight different orbit changes due to changes in RF frequency were measured. By using several sets of input data the uncertainty in the fitted parameters could be estimated.

The mean and standard deviation of the natural energy

Table 1: MAX III Design and Measured Parameters.

	Design [4]	Fitted lattice	Measured
Horizontal beam size at center of D6, σ_x (μm)	-	-	101.0 ± 2.0
Vertical beam size at center of D6, σ_y (μm)	-	-	51.6 ± 2.2
Horizontal beta function at center of D6, β_x (m)	0.27	0.2731 ± 0.0056	-
Vertical beta function at center of D6, β_y (m)	12.8	13.978 ± 0.077	-
Horizontal dispersion at center of D6, η_x (m)	0.14	0.1358 ± 0.0027	0.1341 ± 0.0008
Vertical dispersion at center of D6, η_y (m)	0.00	0.0362 ± 0.0117	0.0278 ± 0.0002
Natural energy spread, σ_E/E	0.0006072	$0.00060005 \pm 0.00000013$	-
Momentum compaction, α_c	0.032559	0.032883 ± 0.000024	-
Horizontal emittance, ϵ_x (nm rad)	13	13.159 ± 0.041	13.7 ± 1.1
Vertical emittance, ϵ_y (nm rad)	-	-	0.170 ± 0.012
Coupling, κ	0.1	-	0.0124 ± 0.0013

spread σ_E/E , momentum compaction α_c , horizontal emittance ϵ_x , the beta functions β_x , β_y and dispersion η_x , η_y at the center of D6, for the 24 fitted lattices, are presented in Table 1.

Dispersion

The dispersion η_i can be determined from the orbit displacement Δi due to a shift in the RF frequency f_{RF} :

$$\eta_i = -\alpha_c \frac{\Delta i}{\Delta f_{RF}} f_{RF}$$

Using the diagnostic beam line the horizontal displacement Δx and vertical displacement Δy at the source point of the diagnostic beam line due to a shift in the RF frequency was determined to be

$$\begin{aligned} \Delta x / \Delta f_{RF} &= -0.04081 \pm 0.00024 \text{ m/MHz} \\ \Delta y / \Delta f_{RF} &= -0.00846 \pm 0.00005 \text{ m/MHz} \end{aligned}$$

The uncertainty of the measurement is given by the uncertainty in determining the magnification factor. With $f_{RF} = 99.925$ MHz and using the fitted momentum compaction, the dispersion at the center of D6 is

$$\begin{aligned} \eta_x &= 0.1341 \pm 0.0008 \text{ m} \\ \eta_y &= 0.0278 \pm 0.0002 \text{ m} \end{aligned}$$

Comparing with the fitted values for the dispersion it can be seen that the values agree, but that the accuracy is significantly better for the diagnostic beam line measurement.

Emittance and Coupling

The emittance ϵ_i is given by

$$\epsilon_i = \frac{\sigma_i^2 - (\sigma_E/E)^2 \eta_i^2}{\beta_i}$$

The horizontal emittance ϵ_x and vertical emittance ϵ_y in MAX III can now be determined using the measurements of the electron beam size and dispersion function at the center of D6 together with the fitted LOCO results for the natural energy spread and the beta function at the center of D6.

$$\epsilon_x = 13.7 \pm 1.1 \text{ nm rad}$$

$$\epsilon_y = 0.170 \pm 0.012 \text{ nm rad}$$

The value used for the energy spread is the fitted natural energy spread. Since the beam size measurement was performed at a low current the actual energy spread is expected to be close to the natural energy spread. However, if there is a discrepancy the actual energy spread is expected to be larger than the natural energy spread, in which case the values for the emittance will be slightly overestimated. The measured horizontal emittance agree with the design value and with the fitted LOCO result.

The emittance coupling ratio in MAX III is

$$\kappa = \epsilon_y / \epsilon_x = 0.0124 \pm 0.0013$$

This value is significantly smaller than the design value of $\kappa = 0.1$. During standard operation a shaker connected to a strip line in the ring excites the vertical tune of the betatron oscillation in order to increase the vertical beam size.

REFERENCES

- [1] G. Kube, in Proceedings of the eighth European Workshop on Diagnostics and Instrumentation for Particle Accelerators, Venice (2007) pp. 6–10.
- [2] O. Chubar, in Proceedings of the 2000 European Particle Accelerator Conference, Vienna (2000) pp. 177–181.
- [3] Å. Andersson, M. Böge, A. Lüdeke, V. Schlott, and A. Streun, Nucl. Instr. and Meth. A 591 (2008) 437.
- [4] M. Sjöström, E. Wallén, M. Eriksson, and L.-J. Lindgren, Nucl. Instr. and Meth. A 601 (2009) 229.
- [5] A. Hansson, E. Wallén, and Å. Andersson, “Transverse electron beam imaging system using visible synchrotron radiation”, submitted for publication.
- [6] O. Chubar and P. Elleaume, in Proceedings of the 1998 European Particle Accelerator Conference, Stockholm (1998), pp. 1177–1179.
- [7] J. Safranek, G. Portmann, A. Terebilo, and C. Steier, in Proceedings of the European Particle Accelerator Conference, EPAC 2002, Paris (2002), pp. 1184–1186.